Transition Met Chem (2010) 35:851–858
DOI 10.1007/s11243-010-9403-9

Crystal structures and magnetic interactions in nickel(II) dibridged complexes formed by both phenolate oxygen-azide, or methanlate groups

Yan Zhang · Xiao-Man Zhang · Tian-Fu Liu · Wen-Guo Xu

Received: 1 June 2010 / Accepted: 16 July 2010 / Published online: 3 August 2010

Abstract Tridentate Schiff base ligands L^1 and L^2, derived from the condensation of 2-hydroxy-3-methoxybenzaldehyde (L) with 2-aminoethanol or 2-aminobutan-1-ol, react with nickel chloride, azide, or thiocyanate to give rise to two dinuclear complexes of formulas $[Ni_2(L)(L^1)_2N_3]\cdot H_2O$ (1), $[Ni_2(L^2)_3(\mu_{1,1}\text{-}N_3)]\cdot 2H_2O$ (2), and one tretranuclear complex $[Ni_2(L^2)_2(NCS)]_2(C_2H_5OH)_2$ (3), where $L^1 = HOCH_2CH(C_2H_5)NCHC_6H_3(O^-)(OCH_3)$ and $L^2 = HO(CH_2)_2NCHC_6H_3(O^-)(OCH_3)$. We have characterized these complexes by analytical, crystal structures, and variable temperature magnetic susceptibility measurements. The magnetic properties of the complexes are studied by magnetic susceptibility (χ_M) vs. temperature measurements. The $\chi_M T$ vs. T plots reveal that compounds 1, 2 and 3 are ferromagnetically coupled.

Introduction

Hetero- and homo-binuclear complexes of Ni(II) have attracted much attention over recent years due to their relevance to the active sites of metalloenzymes [1–4], and potential applications as optical [5, 6], electronic, and molecule-based magnetic materials [7–13]. The structures of the products are dependent on many factors, such as the structure of chelating ligands [14–16], metal centers, anions, and solvents [17]. Numerous papers have so far been published concerning nickel(II) complexes of N-alkyl- and N-aryl-salicylideneimines. When Ni(II) atoms coordinate to these ligands in 1:1 mode, the coordination sphere of Ni(II) remains unsaturated, and the resulting mononuclear coordination moieties can further oligomerize with the aid of bridging groups affording binuclear or polynuclear complexes. Because of the rich coordination modes and an efficient pathway of magnetic exchange, the azido bridge has aroused considerable interest in the past decade. Complexes with novel magnetic properties have been prepared by using this anion, and their magneto-structural correlations have been extensively studied. To date, the azido ligand has been found to bridge metal ions in the modes of $\mu_{1,1}$-(end-on, EO)[18–22], $\mu_{1,3}$-(end-to-end, EE) [23, 24], $\mu_{1,1,3}$ [25–27], $\mu_{1,1,1}$ [28], $\mu_{1,1,1,1}$ [29, 30], $\mu_{1,1,3,3}$ [31, 32] or unusual $\mu_{1,1,1,3,3,3}$ fashions [33] (Scheme 1). Ferromagnetic interactions are usually transmitted by the EO bridging mode of the azido ligand as are antiferromagnetic interactions by the EE bridging mode [34].

Herein, we report the syntheses, crystal structures and magnetic properties of three nickel complexes: two dinuclear Ni(II) complexes with Phenolate Oxygen-Azide bridge $[Ni_2(L)(L^1)_2N_3]\cdot H_2O$ (1) and $[Ni_2(L^2)_3(\mu_{1,1}\text{-}N_3)]\cdot 2H_2O$ (2), and one tetranuclear complex $[Ni_2(L^2)_2(NCS)]_2(C_2H_5OH)_2$ (3). Their magnetic properties have been studied and correlated with molecular structures.

Experimental section

Materials and instrumentation

All chemicals and solvents were of analytical grade and used as received without further purification. The Schiff base (Scheme 2) H_2L^1 was obtained by refluxing an

---

Y. Zhang · X.-M. Zhang · T.-F. Liu (✉) · W.-G. Xu
Department of Chemistry & Key Laboratory of Cluster Science of Ministry of Education, Beijing Institute of Technology, 100081 Beijing, People's Republic of China
e-mail: liutf@bit.edu.cn

Scheme 1 Azide bridging modes

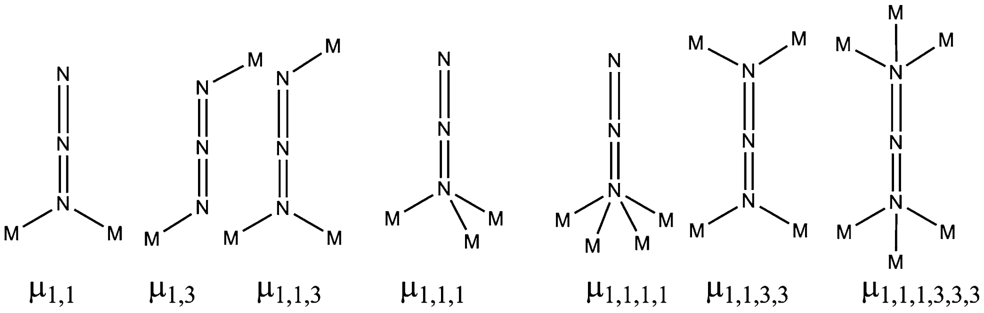

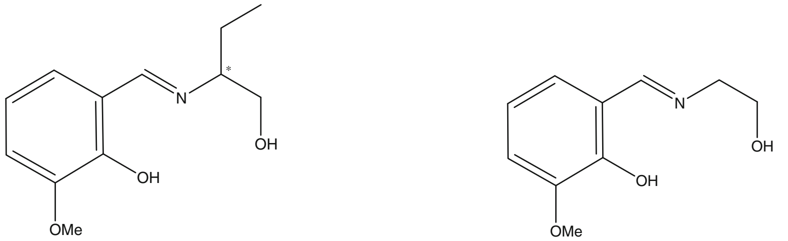

H_2L^1=(*E*)-2-((1-hydroxybutan-2-ylimino)methyl)-6-methoxyphenol **H_2L^2**=(*E*)-2-((2-hydroxyethylimino)methyl)-6-methoxyphenol

Scheme 2 The structures of H_2L^1 and H_2L^2 ligands

ethanolic solution of o-vanillin and racemic 2-aminobutanol for 2 h. The resulting orange–yellow solution containing the Schiff base was used without further purification. The ligand H_2L^2 was prepared by a method similar to that of H_2L^1 by using o-vanillin and racemic 2-ethanolamine. All preparations and manipulations were performed under aerobic conditions. Infrared spectra were recorded as KBr pellets with a Perkin–Elmer Spectrum One FT-IR spectrophotometer in the range 4,000–400 cm^{-1}.

Caution! Azide compounds are potentially explosive! Only a small amount of material should be prepared and handled with care.

Preparation of $[Ni_2(L^1)_2(\mu_{1,1}\text{-}N_3)(\text{o-vanillin})]\cdot H_2O$ (1)

To a solution of H_2L^1 (0.3 mmol) in 6 mL ethanol was added dropwise a solution of $NiCl_2\cdot 6H_2O$ (74.3 mg, 0.3 mmol), and the mixture was stirred for about 1 h at room temperature. Then, an aqueous solution (5 mL) of NaN_3 (0.3 mmol) was added dropwise. After 30 min of stirring, the resulting solution was obtained. The mixture was allowed to stand at room temperature without any further disturbance for several days to give green block crystals. Anal. Calc for $C_{32}H_{41}N_5Ni_2O_{10}$: C, 49.7; H, 5.3; N, 9.1%. Found: C, 51.1; H, 5.1; N, 8.8%. IR (KBr pellet,cm^{-1}): 3,501 br, 2,967 br, 2,932 br, 2,684 w, 2,069 vs, 1,637 vs, 1,601 s, 1,545 m, 1,469 s, 1,442 s, 1,408 m, 1,322 m, 1,240 s, 1,211 vs, 1,167 w, 1,131 br, 1,106 w, 1,077 m, 1,039 w, 975 w, 963 w, 738 s, 604 br.

Preparation of $[Ni_2(L^2)_2(HL^2)(\mu_{1,1}\text{-}N_3)]\cdot 2H_2O$ (2)

The procedure was the same as that for the dimer described above, except for the ligand, for which 6 mL of an ethanolic solution of H_2L^2 (0.3 mmol) was used. Green block crystals were obtained after 10 days. Crystals were filtered out and air-dried. Anal. Calc for $C_{30}H_{42}N_6Ni_2O_{12}$: C, 45.2; H, 5.7; N, 10.6%. Found: C, 45.0; H, 5.6; N, 10.7%. IR (KBr pellet,cm^{-1}): 3,429 br, 2,929 br, 2,833 w, 2,364 br, 2,065 vs, 1,637 vs, 1,601 m, 1,543 br, 1,468 s, 1,445 s, 1,406 m, 1,320 m, 1,302 m, 1,240 s, 1,213 vs, 1,167 w, 1,084 m, 1,054 m, 971 m, 741 s.

Preparation of $[Ni_2(L^2)_2(HL^2)_2(NCS)_2(EtOH)_2]_2\cdot EtOH$ (3)

The procedure was the same as that for the dimer described above, except for the ligand, for which 6 mL of an ethanol solution of H_2L^2 (0.3 mmol) was used. The green reaction mixture was stirred for a few minutes after which a solution of NH_4SCN (34.3 mg, 0.45 mmol) in MeOH (5 mL) was added, and the mixture was stirred for an additional 15 min and filtrated. The resulting filtered was allowed to stand for a few days during which green single crystals were obtained. Anal. Calc for $C_{48.4}H_{66.78}N_6Ni_4O_{16}S_2$: C, 45.1; H, 5.2; N, 6.5%. Found: C, 45.3; H, 5.2; N, 6.7%. IR (KBr pellet,cm^{-1}): 3,406 br, 2,930 br, 2,864 br, 2,104 vs, 1,631 vs, 1,600.85 m, 1,547 w, 1,469 s, 1,443 s, 1,401 m, 1,353 w, 1,319 m, 1,244 s, 1,213 vs, 1,168 w, 1,080 m, 1,056 m, 971 m, 902 br, 856 m, 784 w, 747 s, 637 br.

X-ray crystallography

A single crystal was used for X-ray diffraction analysis. Determination of the unit cell and data collection was performed on a Bruker SMART 1,000× diffractometer using graphite monochromated Mo-K_α radiation at 293(2) K. The structure was solved by direct methods in SHELXS-97 [35] and refined using a full-matrix least squares procedure on F^2 in SHELXS-97 [36]. The disordered C_{17}, $C_{18,}$ C_{19}, N_2 and O_6 sites were refined with an equal occupation factor of 0.5; and C_{22} was refined with three positions with occupation factor of 0.419, 0.384 and 0.197; and C_{23}, C_{24} and O_8 were refined with the occupation factor of 0.556 and 0.444 for compound **3**. All H atoms could be located in the difference Fourier map and refined without constraints.

Magnetic measurements

Magnetic data were recorded using a Quantum Design SQUID magnetometer. To avoid orientation in the magnetic field, the samples were pressed in a home-made Teflon sample holder equipped with a piston. The data were corrected for diamagnetism of the constituent atoms using Pascal's constants.

Results and discussion

Description of the crystal structures

[$Ni_2(L^1)_2(\mu_{1,1}$-$N_3)$(o-vanillin)]·H_2O

Single-crystal X-ray diffraction of **1** (Fig. 1) reveals that it crystallizes in the triclinic space group P $\bar{1}$, and the structure is presented in Table 1. The structure of the molecular unit is shown in Fig. 1a. Selected bond lengths and angles of complex **1** are collated in Table 2. The unit includes one independent dimeric complex molecule and one crystal water. The complex has a dinickel(II) structure with one azide group in end-on fashion through N_3 and one deprotonated μ_2-phenolate oxygen atom O_5 of *o*-vanillin bridges. Each nickel(II) atom is coordinated to one ligand H_2L^1 (Scheme 1a), which acts in a tridentate mode, with one amino N, one deprotonated phenoxo O atom and one ethanol O atom coordinated. The remaining alkoxyl O atom of H_2L^1 is left noncoordinated in a neutral form. One *o*-vanillin molecule is contained, with aldehyde oxygen atom O_4 coordinated to Ni_1 and alkoxyl O_6 atom coordinated to Ni_2. The basal bond distances around the Ni_1 atom are in the 2.111(9)–1.997(5) Å range, and the apical bond distances are 2.084(5) and 2.146(3) Å, respectively. The bond distances around the Ni_2 atoms are in the 2.124(1)–1.992(1) Å range, and the apical bond distances are 2.099(9) and 2.219(2) Å. The axial bond angle O_4-Ni_1-N_3 has a small value of 163.32(9)°, and the other axial bond angle O_6-Ni_2-N_3 has a smaller value of 152.41(7)°, indicating severe distortions of the octahedral configurations. The major distortion from a "regular" octahedron for two nickel centers could be the result of the bridging azide and phenolate group. The largest bond between Ni_2 and O_6 is most probably due to the bonding of the phenolate oxygen atom of the same ring and to the coordination of hydroxyl group. The bridging O_5 atom has almost equivalent bond lengths of 2.022(9) and 2.016(2) Å with Ni_1 and Ni_2, respectively. The bridging N_3 atom has slightly longer bond lengths of 2.146(3) and 2.099(9) Å with Ni_1 and Ni_2. Ni_1-O_5-Ni_2 bridging angle is 104.63(7)°, and Ni_1-N_3-Ni_2 bridging angle is 97.66(5)°. The nickel(II) centers are separated by 3.196(7) Å.

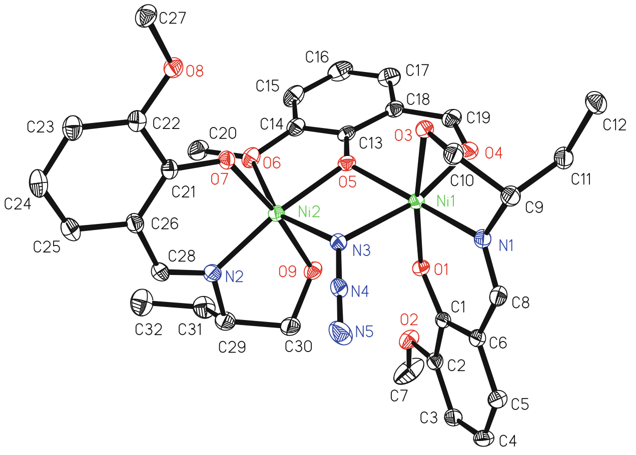

Fig. 1 The molecular structure (30% thermal probability ellipsoids) of complex **1** showing the atom numbering (hydrogen atoms and waters are omitted for clarity)

[$Ni_2(L^2)_2(HL^2)(\mu_{1,1}$-$N_3)$]·2$H_2O$

The crystal structure of complex 2 includes one independent dimeric complex molecule and two H_2O molecules (Fig. 2). Selected bond lengths and angles of complex **2** are collated in Table 3. The dinuclear unit is formed by two Ni(II) atoms labeled Ni_1 and Ni_2, bridged by one azide group in end-on fashion through N_6 and one μ_2-phenolate oxygen atom O_1 of the Schiff base. The coordination sites of the octahedral Ni_1 atom are completed by one nitrogen atom N_2 and two oxygen atoms O_4 and O_9 of the same Schiff base ligand and by a nitrogen atom N_3 of the bridging moiety. Similarly, the remaining sites of distorted octahedral geometry of Ni_2 atom are occupied by one nitrogen atom N_1 and two oxygen atoms O_5 and O_7 of the same Schiff base ligand and a methoxy oxygen atom O_2 of the bridging Schiff base. Deviation of the Ni_1 and Ni_2

Table 1 Crystal data and details of the structure determination

Compound Formula	1 $C_{32}H_{41}N_5Ni_2O_{10}$	2 $C_{30}H_{42}N_6Ni_2O_{12}$	3 $C_{48.4}H_{66.78}N_6Ni_4O_{16}S_2$
Mr[g mol^{-1}]	773.08	796.12	1287.56
T[K]	293(2)	293(2)	77(2)
λ[Å]	0.71073	0.71073	0.71073
Crystal system	Triclinic	Triclinic	Monoclinic
Space group	$P\bar{1}$	$P\bar{1}$	C_2/c
a[Å]	10.315(2)	10.140(2)	24.660(5)
b[Å]	12.766(2)	11.456(2)	19.636(4)
c[Å]	13.781(2)	15.398(3)	11.314(2)
α[°]	71.999(5)	91.47(3)	90
β[°]	76.521(5)	96.10(3)	90.957(3)
γ[°]	85.040(5)	96.05(3)	90
V[$Å^3$]	1678.2(5)	1767.4(6)	5477.6(2)
Z	2	2	8
ρ_{calcd} [g cm^{-3}]	1.530	1.458	1.561
μ [mm^{-1}]	1.187	1.130	1.503
F(000)	808	832	2,685
Crystal size [mm]	0.33 × 0.30 × 0.23	0.12 × 0.10 × 0.08	0.33 × 0.23 × 0.20
θ[°]	3.07–27.48	1.79–25.30	3.19–27.47
Measured reflections	13,646	10,155	22,173
Unique reflection	7,384	6,879	6,181
R(int.)	0.0251	0.0174	0.0315
Completeness [%]	95.7 ($\theta = 27.48$)	97.9 ($\theta = 25.30$)	98.4($\theta = 27.47$)
Data/restaints/parameters	7,384/1/463	6,879/6/479	6,181/33/433
GOF on F2	0.998	1.008	0.997
$R_1[I > 2\sigma(I)]$	0.0477	0.0554	0.0489
w$R_2[I > 2\sigma(I)]$	0.1191	0.1534	0.1207
R_1 (all data)	0.0569	0.0867	0.0558
wR_2 (all data)	0.1126	0.1671	0.1269
Largest diff. peak and hole [e$Å^{-3}$]	0.81, −0.69	0.87, −0.52	0.96, −0.93

atoms from the mean plane formed by the three oxygens and one nitrogen atom of Ni_1 and by one nitrogen and three oxygen atoms of Ni_2 are 0.0768 and 0.0377 Å, respectively. The basal bond distances around the Ni_1 atom are in the 2.116(3)–1.980(5) Å range, and the apical bond distances are 2.091(9) and 2.190(4) Å, respectively considering the bond angle N_3-Ni_1-N_6 = 166.09(1)°. The bond distances around the Ni_2 atom are in the 2.154–1.979 Å range. The apical bond distances are 2.088(0) and 2.240(0) Å considering the bond angle O_2-Ni_2-N_6 = 152.47(0)°. The major distortion could arise from the same reason as complex **1**. Ni_1-O_1-Ni_2 bridging angle is 106.36(1)° and Ni_1-N_6-Ni_2 bridging angle is 96.21(2)°.The distance between Nickel(II) centers is 3.184(9) Å.

$[Ni_2(L^2)_2(HL^2)_2(NCS)_2(EtOH)_2]_2{\cdot}EtOH$

Compound **3** crystallizes in the monoclinic space group C_2/c, and the molecular structure is shown in Fig. 3. Selected bond lengths and angles of complex **3** are collated in Table 4. The centrally symmetric unit includes one independent tetranuclear complex molecule and one ethanol molecule as crystallization solvent. The complex molecule consists of an arrangement of four nickel atoms, four deprotonated accessory ligands and four terminal monodentate ligands (two NCS^- and two methanol molecules). Four Ni and four O atoms including two phenolate O atoms (O_3 and O_3A) and two alkoxide O atoms (O_4 and O_4A) occupy the vertices of a distorted $\{Ni_4(\mu_3\text{-}O)_4\}$ cubane core. Ni_1 and Ni_1A are arranged in the same manner, the coordination sphere of each completed by three bridging O atoms, one phenolate O atoms, one alkoxyl O atom and one amino N atom from $(L_2)^{2-}$ and with the Ni-O bond length in the range of 1.980(2)–2.292(2) Å and Ni-N bond length of 1.977(2)Å. Ni_2 and Ni_2A are in the same coordination sphere, including three bridging O atoms, one O atom from the methanol ligand, one amino N atom from $(HL^2)^-$ and one N atom from NCS^- with the

Table 2 Selected bond lengths (Å) and angles (deg) for compound **1**

Ni(1)-O(1)	1.998(2)	Ni(2)-O(7)	1.993(2)
Ni(1)-N(1)	2.001(3)	Ni(2)-N(2)	1.993(3)
Ni(1)-O(5)	2.022(2)	Ni(2)-O(5)	2.017(2)
Ni(1)-O(4)	2.085(2)	Ni(2)-N(3)	2.100(2)
Ni(1)-O(3)	2.112(2)	Ni(2)-O(9)	2.124(2)
Ni(1)-N(3)	2.146(2)	Ni(2)-O(6)	2.219(2)
Ni(2)-N(3)-Ni(1)	97.66(10)	Ni(2)-O(5)-Ni(1)	104.61(9)
O(1)-Ni(1)-N(1)	91.30(9)	O(7)-Ni(2)-N(2)	91.51(9)
O(1)-Ni(1)-O(5)	95.81(8)	O(7)-Ni(2)-O(5)	102.02(8)
N(1)-Ni(1)-O(5)	170.24(9)	N(2)-Ni(2)-O(5)	165.34(9)
O(1)-Ni(1)-O(4)	91.24(8)	O(7)-Ni(2)-N(3)	95.51(9)
N(1)-Ni(1)-O(4)	99.58(10)	N(2)-Ni(2)-N(3)	107.02(10)
O(5)-Ni(1)-O(4)	86.97(9)	O(5)-Ni(2)-N(3)	77.56(9)
O(1)-Ni(1)-O(3)	171.28(8)	O(7)-Ni(2)-O(9)	171.15(8)
N(1)-Ni(1)-O(3)	80.48(9)	N(2)-Ni(2)-O(9)	80.56(9)
O(5)-Ni(1)-O(3)	92.70(8)	O(5)-Ni(2)-O(9)	85.53(8)
O(4)-Ni(1)-O(3)	87.30(8)	N(3)-Ni(2)-O(9)	90.60(9)
O(1)-Ni(1)-N(3)	91.11(9)	O(7)-Ni(2)-O(6)	87.59(8)
N(1)-Ni(1)-N(3)	96.84(10)	N(2)-Ni(2)-O(6)	100.28(10)
O(5)-Ni(1)-N(3)	76.39(9)	O(5)-Ni(2)-O(6)	74.98(8)
O(4)-Ni(1)-N(3)	163.35(9)	N(3)-Ni(2)-O(6)	152.41(9)
O(3)-Ni(1)-N(3)	92.74(9)	O(9)-Ni(2)-O(6)	89.95(8)

Table 3 Selected bond lengths (Å) and angles (deg) for compound **2**

Ni(2)-N(1)	1.979(5)	Ni(1)-O(1)	1.987(3)
Ni(2)-O(5)	1.989(3)	Ni(1)-N(2)	1.981(4)
Ni(2)-O(1)	1.992(4)	Ni(1)-O(4)	2.017(4)
Ni(2)-N(6)	2.088(4)	Ni(1)-N(3)	2.092(5)
Ni(2)-O(7)	2.154(3)	Ni(1)-O(9)	2.117(4)
Ni(2)-O(2)	2.240(4)	Ni(1)-N(6)	2.190(4)
Ni(2)-N(6)-Ni(1)	96.21(16)	Ni(1)-O(1)-Ni(2)	106.36(14)
N(1)-Ni(2)-O(5)	90.99(17)	O(1)-Ni(1)-N(2)	168.03(17)
N(1)-Ni(2)-O(1)	165.65(17)	O(1)-Ni(1)-O(4)	95.64(14)
O(5)-Ni(2)-O(1)	103.33(15)	N(2)-Ni(1)-O(4)	91.62(17)
N(1)-Ni(2)-N(6)	101.47(17)	O(1)-Ni(1)-N(3)	89.76(17)
O(5)-Ni(2)-N(6)	94.49(16)	N(2)-Ni(1)-N(3)	99.30(18)
O(1)-Ni(2)-N(6)	78.73(14)	O(4)-Ni(1)-N(3)	93.57(18)
N(1)-Ni(2)-O(7)	79.83(17)	O(1)-Ni(1)-O(9)	92.14(15)
O(5)-Ni(2)-O(7)	170.33(14)	N(2)-Ni(1)-O(9)	80.51(17)
O(1)-Ni(2)-O(7)	85.83(15)	O(4)-Ni(1)-O(9)	172.13(14)
N(6)-Ni(2)-O(7)	90.32(15)	N(3)-Ni(1)-O(9)	87.67(18)
N(1)-Ni(2)-O(2)	105.66(17)	O(1)-Ni(1)-N(6)	76.42(14)
O(5)-Ni(2)-O(2)	89.68(14)	N(2)-Ni(1)-N(6)	94.18(16)
O(1)-Ni(2)-O(2)	73.83(14)	O(4)-Ni(1)-N(6)	89.48(16)
N(6)-Ni(2)-O(2)	152.46(16)	N(3)-Ni(1)-N(6)	166.08(18)
O(7)-Ni(2)-O(2)	89.92(14)	O(9)-Ni(1)-N(6)	91.16(15)

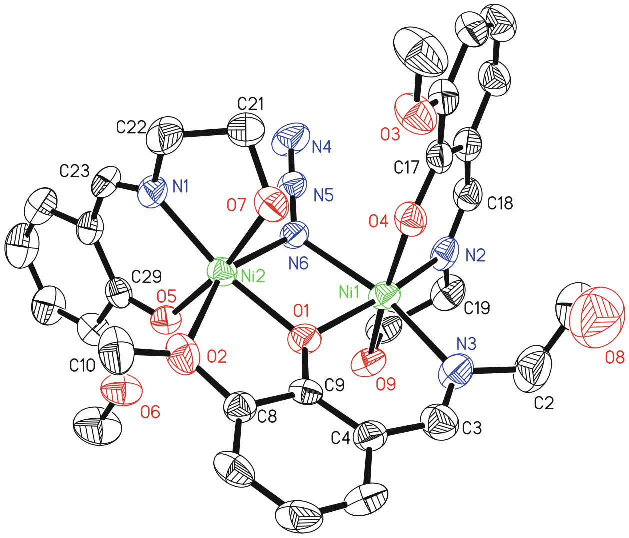

Fig. 2 The molecular structure (30% thermal probability ellipsoids) of complex **2** showing the atom numbering (hydrogen atoms and waters are omitted for clarity)

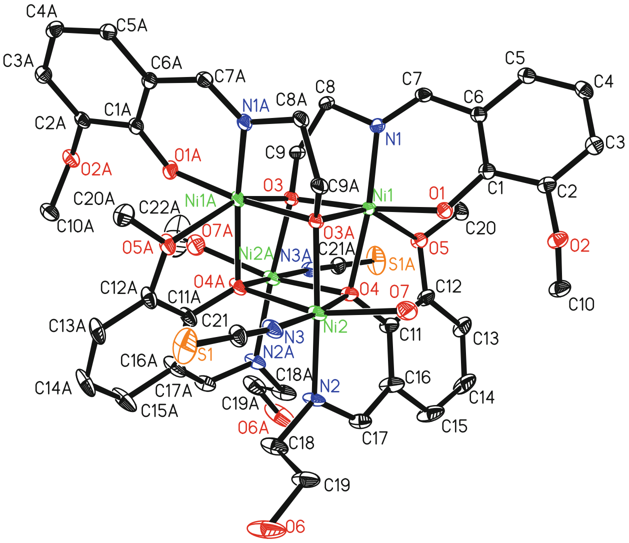

Fig. 3 The molecular structure (30% thermal probability ellipsoids) of complex **3** showing the atom numbering (only one position of disorder atoms C_{17}, C_{18}, C_{19}, N_2 and O_6 are shown, hydrogen atoms and ethanol molecule are omitted for clarity). Symmetry transformations used to generate equivalent atoms: #A $-x+1, y, -z+3/2$

Ni-O and Ni-N bond lengths in the range of 2.014(2)–2.101(3) and 1.992(3)–2.053(3) Å. Among the Ni-O distances corresponding to the oxygen atoms that belong to the cubane core, Ni$_2$-O$_4$A (2.275(3)Å) and Ni$_2$A-O$_4$ (2.275(3)Å) are slightly longer than other two Ni-O bonds ranging from 2.014(2) to 2.074(2)Å. In this elongated cube, the distance of 3.0574(6) Å between Ni1 and Ni$_2$ equal to the distance between Ni$_1$A and Ni$_2$A is the shortest, and the distance of 3.3890(9) Å between Ni$_2$ and Ni$_2$A is the longest. The main distortion of the cubane core is also due to the differences in Ni-O-Ni angles which average 103.93° in

Table 4 Selected bond lengths (Å) and angles (deg) for compound **3**

Ni(1)-N(1)	1.977(2)	Ni(2)-N(3)	1.992(3)
Ni(1)-O(1)	1.980(2)	Ni(2)-O(4)	2.014(2)
Ni(1)-O(3)	2.040(2)	Ni(2)-O(3)#1	2.0520(19)
Ni(1)-O(4)	2.042(2)	Ni(2)-N(2)	2.053(3)
Ni(1)-O(3)#1	2.074(2)	Ni(2)-O(7)	2.101(3)
Ni(1)-O(5)	2.292(2)	Ni(2)-O(4)#1	2.275(3)
N(1)-Ni(1)-O(1)	92.27(9)	N(1)-Ni(1)-O(3)	83.56(9)
O(1)-Ni(1)-O(3)	172.54(8)	N(1)-Ni(1)-O(4)	160.28(11)
O(1)-Ni(1)-O(4)	103.06(9)	O(3)-Ni(1)-O(4)	82.42(9)
N(1)-Ni(1)-O(3)#1	110.78(9)	O(1)-Ni(1)-O(3)#1	93.66(9)
O(3)-Ni(1)-O(3)#1	82.11(9)	O(4)-Ni(1)-O(3)#1	80.91(8)
N(1)-Ni(1)-O(5)	96.19(8)	O(1)-Ni(1)-O(5)	86.24(9)
O(3)-Ni(1)-O(5)	100.32(8)	O(4)-Ni(1)-O(5)	72.87(7)
O(3)#1-Ni(1)-O(5)	153.01(7)	N(3)-Ni(2)-O(4)	173.00(11)
N(3)-Ni(2)-O(3)#1	94.78(9)	O(4)-Ni(2)-O(3)#1	82.12(8)
N(3)-Ni(2)-N(2)	96.2(3)	O(4)-Ni(2)-N(2)	85.9(3)
O(3)#1-Ni(2)-N(2)	165.8(4)	N(3)-Ni(2)-N(2')	93.6(3)
O(4)-Ni(2)-N(2')	89.7(3)	O(3)#1-Ni(2)-N(2')	171.6(3)
N(2)-Ni(2)-N(2')	10.2(8)	N(3)-Ni(2)-O(7)	97.21(11)
O(4)-Ni(2)-O(7)	88.94(10)	O(3)#1-Ni(2)-O(7)	87.25(9)
N(2)-Ni(2)-O(7)	100.1(5)	N(2')-Ni(2)-O(7)	90.7(5)
N(3)-Ni(2)-O(4)#1	97.76(10)	O(4)-Ni(2)-O(4)#1	75.45(9)
O(3)#1-Ni(2)-O(4)#1	76.65(8)	N(2)-Ni(2)-O(4)#1	93.0(5)
N(2')-Ni(2)-O(4)#1	103.2(5)	O(7)-Ni(2)-O(4)#1	158.83(8)
Ni(1)-O(3)-Ni(2)#1	103.61(9)	Ni(1)-O(3)-Ni(1)#1	97.46(9)
Ni(2)#1-O(3)-Ni(1)#1	95.62(8)	Ni(2)-O(4)-Ni(1)	97.83(9)
Ni(2)-O(4)-Ni(2)#1	104.23(9)	Ni(1)-O(4)-Ni(2)#1	96.16(9)

Symmetry transformations used to generate equivalent atoms: #1 $-x+1, y, -z+3/2$

the case of Ni_1-O_3-Ni_2A and Ni_2-O_4-Ni_2A while the other Ni-O-Ni angles are around 95.63–97.84°.

Magnetic measurements

The magnetic susceptibilities of complexes **1** and **2** shown in Fig. 4 were measured at 0.1 T in the temperature range 2.0–300 K for **1** and 5.0–300 K for **2**. **1** and **2** exhibit the similar magnetic properties. Plots of $\chi_M T$ vs. T for **1** and 2 (Fig. 4) show typical ferromagnetic behaviors: an increase in the effective magnetic moment with decreasing temperature. The $\chi_M T$ product at 300 K (2.77 cm^3 mol^{-1} K for **1** and 2.92 cm^3 mol^{-1} K for **2**) is on the order of the expected one for two uncoupled Ni(II) ions, with g about 2.2, and this value increases upon cooling to reach a maximum at 30 K (3.32 cm^3 mol^{-1} K) for 1 (31 K (3.35 cm^3 mol^{-1} K) for **2**) then diminishes with decreasing temperature. This behavior with the decrease in $\chi_M T$ at low temperatures is attributed to either interdinuclear antiferromagnetic interactions and/or the effect of the zero-field splitting (ZFS) of the $S = 1$ ground state. The cryomagnetic behavior of **1** and **2** obeys the Curie–Weiss law in the temperature region 50–300 K, yielding $C = 2.72$ cm^3 K mol^{-1}, $\theta = 8.02$ K for **1** and $C = 2.76$ cm^3 K mol^{-1}, $\theta = 8.11$ K for **2**.

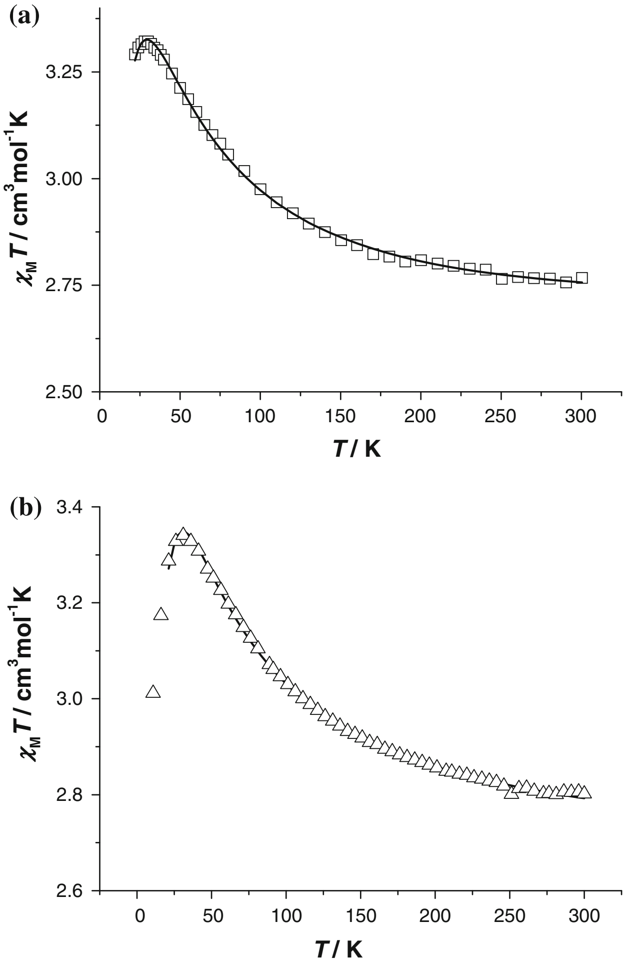

Fig. 4 **a** Plot of $\chi_M T$ vs. T for **1**. **b** Plot of $\chi_M T$ vs. T for **2**. The *solid line* represents the best fit of the experimental data

The experimental data were fitted with the following expression, derived from the Van Vleck formula ($H = -JS_1S_2$) for two S = 1 ions and modified for inclusion of the zero-field splitting parameter (D) in the ground state.

$$\chi_M T = \frac{Ng^2\beta^2}{3k} f(x) + \mathrm{TIP}T. \qquad (1)$$

with

$$f(x) = \frac{2e^{-2J/kT} + 6e^{D/kT} + 24e^{-2D/kT}}{3e^{-2J/kT} + e^{-3J/kT} + e^{2D/kT} + 2e^{D/kT} + 2e^{-2D/kT}}$$

where the symbols have their usual meaning, and the last term (TIP) is the temperature-independent paramagnetism.

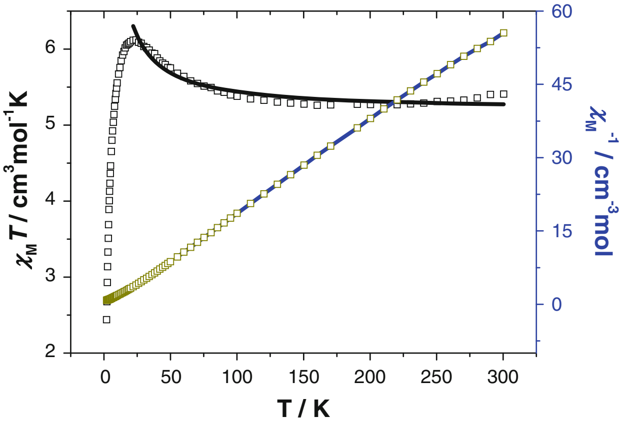

Fig. 5 Plot of χ_M^{-1} vs. T and $\chi_M T$ vs. T for **3**. The *solid line* represents the best fit of the experimental data

The best least squares fitting was obtained with $J = + 18.45$ cm^{-1}, $g = 2.39$, $D = 2.27$ cm^{-1}, and TIP $= 2.17 \times 10^{-4}$ cm^3 mol^{-1} with $R = 4.48 \times 10^{-6}$ for **1**; $J = + 17.09$ cm^{-1}, $g = 2.44$, $D = 2.59$ cm^{-1}, and TIP $= -1.24 \times 10^{-5}$ cm^3 mol^{-1} with $R = 3.25 \times 10^{-6}$ for **2** (R value is defined as $\sum\left[(\chi_M)_{obs} - (\chi_M)_{calc}\right]^2 / \sum\left[(\chi_M)_{obs}\right]^2$). The positive J values demonstrate that Ni(II) spins are coupled ferromagnetically.

The magnetic susceptibilities of complexes **3** shown in Fig. 5 were measured at 0.1 T in the temperature range 2.0–300 K. It also onsets ferromagnetic coupling between Ni ions. The cryomagnetic behavior of **3** obeys the Curie–Weiss law in the temperature region 50–300 K with $C = 5.28$ cm^3 K mol^{-1}, $\theta = 1.8$ K.

The data were analyzed by using the spin Hamiltonian (Eq. 1), where J_A characterizes the exchange interactions Ni_1-Ni_2A and Ni_2-Ni_2A with larger Ni-O-Ni angles, while J_B characterizes the remaining four pairwise interactions (Fig. 6).

$$\hat{H} = -2J_A(\hat{S}_1 \cdot \hat{S}_2 + \hat{S}_2 \cdot \hat{S}_3) - 2J_B(\hat{S}_1 \cdot \hat{S}_3 + \hat{S}_1 \cdot \hat{S}_4 + \hat{S}_3 \cdot \hat{S}_4 + \hat{S}_2 \cdot \hat{S}_4). \quad (1)$$

Thereafter, a 'two J' mode is employed to analyze the Ni_4 cluster (Ni-J_1-Ni-J_2-Ni-J_1-Ni) [37]. A least squares fit to the data leads to $g = 2.27$, $J_A = -1.26$ cm^{-1}, $J_B = 1.92$ cm^{-1}, TIP $= 1 \times 10^{-5}$ cm^3 mol^{-1}, $R = 1.21 \times 10^{-6}$ ($R = \sum\left[(\chi_M)_{obs} - (\chi_M)_{calc}\right]^2 / \sum\left[(\chi_M)_{obs}\right]^2$). The negative J_A and positive J_B are in good agreement with the structural feature described above.

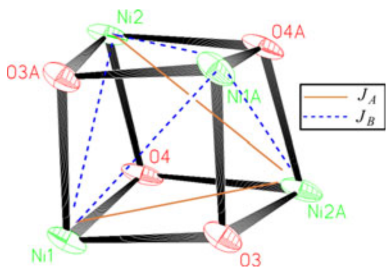

Fig. 6 Topology of the exchange coupling constants in the Ni_4O_4 cube of 3

Tetranuclear Ni_4O_4 cubane complexes have proven to be a class of complexes with highly interesting magnetic properties. In most cases, the superexchange interaction is predominantly ferromagnetic, leading to a high-spin ($S = 4$) ground state. The intramolecular magnetic interactions are closely related to the Ni-O-Ni angles; they are ferromagnetic for angles close to orthogonality and antiferromagnetic for larger angles.

Concluding remarks

The Schiff bases L^1 and L^2 contain three separate binding subunits, each being able to coordinate one metal ion and the phenol group; in their deprotonated forms, they have a strong tendency to bridge the two metal ions. For this reason, the two metal ions are forced to remain close to each other, and the phenolate group plays a key role in determining the molecular geometry of the binuclear species. Moreover, because of the number of binding sites, the ligand does not completely saturate the coordination sites of the metal ions and the complexes formed can be used to assemble at least one secondary ligand. This capability is well illustrated in the crystal structures obtained here using Ni(II) metal ions. In all cases, the Ni-Ni bond distances are very close to each other. The magnetic behavior of compounds **1**–**3** depends on the pseudohalide and methanolate ligand which bridges the two nickel (II) atoms. The $\chi_M T$ vs. T plots reveal that compounds 1, 2 and 3 are ferromagnetically coupled.

Supplementary material

CCDC 755211–755213 contain the supplementary crystallographic data for compounds 1, 2 and 3, respectively. These data can be obtained free of charge from The Cambridge Crystallographic Data Centre via www.ccdc.cam.ac.uk/data_request/cif.

Acknowledgments We are grateful for financial support from the Natural Science Foundation Council of China (NSFC) (grant No. 20401003) and 111 Project (B07012).

References

1. Holm RH, Ciurli S, Weigel JA (1990) Prog Inorg Chem 38:1
2. Solomon EI, Lowery MD (1993) Science 259:1575

3. Sellmann D (1993) Angew Chem Int Ed Engl 32:64
4. Wu JZ, De Angelis F, Carrell TG, Yap GPA, Sheats J, Car R, Dismukes GC (2006) Inorg Chem 45:189
5. Lai SW, Cheung KK, Chan MCW, Che CM (1998) Angew Chem Int Ed 37:182
6. Burns MC, Tershansy MA, Ellsworth JM, Khaliq Z, Peterson L Jr, Smith MD, zur Loye H-C (2006) Inorg Chem 45:10437
7. Gatteschi D, Kahn O, Palacio F (eds) (1991) Materials magnetic molecular NATO ASI Series E 198. Kluwer, Dordrecht
8. Winpenny REP (2001) Adv Inorg Chem 52:1
9. Stamatatos TC, Abboud KA, Wernsdorfer W, Christou G (2007) Angew Chem Int Ed 46:884
10. Raptis RG, Georgakaki IP, Hockless DCR (1999) Angew Chem Int Ed 38:1634
11. Fabre M, Bonvoisin J (2007) J Am Chem Soc 129:1434
12. Rohmer MM, Liu IPC, Lin JC, Chiu MJ, Lee CH, Lee GH, Benard M, Lopez X, Peng SM (2007) Angew Chem Int Ed 46:3533
13. Xie YS, Liu QL, Jiang H, Du CX, Xu XL, Yu MG, Zhu Y (2002) New J Chem 26:176
14. Isele K, Franz P, Ambrus C, Bernardinelli G, Decurtins S, Williams AF (2005) Inorg Chem 44:3896
15. Bagai R, Datta S, Betancur-Rodriguez A, Abboud KA, Hill S, Christou G (2007) Inorg Chem 46:4535
16. Chichak KS, Cantrill SJ, Pease AR, Chiu SH, Cave GWV, Atwood JL, Stoddart JF (2004) Science 304:1308
17. Paine TK, Rentschler E, Weyhermuller T, Chaudhuri P (2003) Eur J Inorg Chem 3167
18. Godbole MD, Roubeau O, Mills AM, Kooijman H, Spek AL, Bouwman E (2006) Inorg Chem 45:6713
19. Lee CS, Wu CY, Hwang WS, Dinda J (2006) Polyhedron 25:1791
20. Ronson TK, Adams H, Ward MD (2005) Eur J Inorg Chem 4533
21. Yang EC, Wernsdorfer W, Hill S, Edwards RS, Nakano M, Maccagnano S, Zakharov LN, Rheingold AL, Christou G, Hendrickson DN (2003) Polyhedron 22:1727
22. Escuer A, Font-Bardy′a M, Kumar SB, Solans X, Vicente R (1999) Polyhedron 18:909
23. Koner S, Saha S, Mallah T, Okamoto K-I (2004) Inorg Chem 43:840
24. Zhang Y, Wang XT, Zhang XM, Liu TF, Xu WG, Gao S (2010) Inorg Chem 49:5868
25. Domı′nguez-Vera JM, Sua′rez-Varela J, Maimoun IB, Colacio E (2005) Eur J Inorg Chem 1907
26. Monfort M, Resino I, Ribas J, Solans X, Font-Bardia M, Stoeckli-Evans H (2002) New J Chem 26:1601
27. Murugesu M, Habrych M, Wernsdorfer W, Abboud KA, Christou G (2004) J Am Chem Soc 126:4766
28. Ghoshal D, Maji TK, Zangrando E, Mallah T, Rivie‘re EÄ, Chaudhuri NR (2004) Inorg Chim Acta 357:1031
29. Karmakar TK, Chandra SK, Ribas J, Mostafa G, Lu TH, Ghosh BK (2002) Chem Commun 2364
30. Goher MAS, Cano J, Journaux Y, Abu-Youssef MAM, Mautner FA, Escuer A, Vicente R (2000) Chem-Eur J 6:778
31. Papaefstathiou GS, Perlepes SP, Escuer A, Vicente R, Font-Bardia M, Solans X (2001) Angew Chem Int Ed 40:884
32. Papaefstathiou GS, Escuer A, Vicente R, Font-Bardia M, Perlepes SP, Solans X (2001) Chem Commun 23:2414
33. Meyer F, Kircher P, Pritzkow H (2003) Chem Commun 6:774
34. Mialane P, Dolbecq A, Marrot J, Rivie‘re E, Se′cheresse F (2005) Chem Eur J 11:1771
35. Sheldrick GM (1990) SHELXS-97, program for the solution of crystal structures. University of Gottingen, Germany
36. SheldrickGM (1997) SHELXS-97, program for the refinement of crystal structures. University of Gottingen, Germany
37. MAGMUN4.1/OW01.exe is available as a combined package free of charge from the authors (http://www.ucs.mun.ca/lthomp/magmun). MAGMUN has been developed by Dr Zhiqiang Xu and OW01.exe by Dr O. Waldmann